(NASA-CR-173817) REAL JET EFFECTS ON DUAL JETS IN A CROSSFLOW Semiannual Report (Virginia Polytechnic Inst. and State Univ.) 18 p HC A02/MF A01 CSCL 20D

N84-29161

Unclas
G3/34 20056

COLLEGE OF ENGINEERING

VIRGINIA POLYTECHNIC INSTITUTE AND STATE UNIVERSITY

BLACKSBURG, VIRGINIA

Semi-Annual Report
NASA NAG 2-256

Aug. 1984

Real Jet Effects on Dual Jets in a Crossflow

Joseph A. Schetz

Aerospace and Ocean Engrg. Dept.

BACKGROUND

The jet in a crossflow flow problem is of interest in a number of situations from jet-powered V/STOL aircraft to smoke stacks. The available information on this flow, in general, is discussed in Ref. (1). For the V/STOL application, the pressure field induced on adjacent surfaces is of particular importance, so there have been a number of detailed experimental studies of that part of the flowfield covering many of the important variables and parameters (see Refs. (2) - (12)). Reviews of the early work can be found in Refs. (13) and (14), and a tabulation of all but the most recent information is in Ref. (15). The jet induces negative (with respect to the freestream) pressures on the nearby surfaces, and this results in a net loss of lift on the body viewed as a whole. The longitudinal variation of the surface pressures is also important, since that determines the resulting pitching moment.

Until recently, there were four aspects of the general problem that had received little or no careful study. The first was the effect of the angle of the jet with respect to the crossflow. That is important because the transition to wingborne operation is commonly accompanied by a change in the angle of the jet thrust vector. There are few prior investigations in the literature (see Refs. (8), (11) and (16)). The second item is the performance of dual-jet configurations, either in-line or side-by-side. The mutual interference as a function of center-to-center spacing is the issue here. Again, few references (e.g. Refs. (3), (8) and (17)) exist. The third item is the behavior of a jet (or jets) injected from a body of revolution as opposed to the large flat plates usually considered. This is of obvious importance for V/STOL aircraft with lifting jets in the fuselage. One can anticipate substantial transverse pressure "relief" around a cylindrical body. The only early work was in Ref. (18) which considered a case were $D_{jet}/D_{body} << 1$. That is not realistic for V/STOL aircraft where $D_{jet}/D_{body} \approx 1/2$ can be encountered. The fourth item concerns so-called "real jet" effects, i.e. the effects of non-uniform and/or non-circular jet exhaust profiles. Most practical devices operate in the presence of such phenomena and some early studies have shown the influences to be rather large (Ref. (12)). A recent study by the writer and co-workers at NASA Ames has investigated the first three items outlined above in some detail (Ref. (19)). The current work is, therefore, aimed at the fourth item above.

There have also been a number of analyses and semi-empirical analyses for the jet in a crossflow problem (e.g. Refs. (15), (20) - (29) that should be mentioned in a discussion of this general flow. None of them, however, can presently treat in a fundamental way the combination of two or more of the items described here. Hopefully, the experimental studies proposed will aid in the generalization of the existing analyses.

PROGRESS REPORT

Starting in October 1983, the Department of Aerospace and Ocean Engineering at VPI has engaged into a wind tunnel study of dual jets in a cross flow using the Dual-Jet Flat Plate Model built at NASA Ames. The study is aimed at exploring the effects of non-uniform jet exhaust profiles on the pressure field induced on the nearby surface.

In order to fit the 7 ft.-wide NASA model into the 6 x 6 ft. test section of our wind tunnel and to adapt the model to our air supply system, a segment of the test-section side wall has been modified so as to allow the Flat Plate Model to protrude 1 ft. through a sealed cutout. Fig. 1 shows the Dual-Jet Flat Plate Model installed in the test section.

Each injector is supplied with air from two independently regulated DC-driven blowers; a smaller, 300 cfm blower provides the air for the central core of the jet (through a central tube) and the larger, 1400 cfm blower provides the air for the outer annulus. By controlling the blower speeds and extension of the central tube we can vary the nozzle exit profile over a wide range of shapes. This allows us to obtain exit profiles representative of various practical installations. Fig. 2 presents examples of exit profiles obtained at 90° injection angle.

The basic instrumentation for the present experiments consists of twelve 48-port Scanivalves, Fluid Wafer Switches and 1 PSIA PDCR 22 pressure transducers. All the surface pressure data as well as other measurements necessary to define test and flow conditions are recorded and processed by the H-P 3052A Data Acquisition System and the HP 9836 Computer. To assure high accuracy, the transducer calibration is updated after each Scanivalve scan, and stepping from one pressure tap to the next one is interactively controlled by the computer so as to allow sufficient time for the pressure to fully stabilize.

The tests completed to data have obtained detailed surface pressure measurements for 90^{0} circular injectors producing exit profiles representative of turbofan nozzles (such as TF-34 nozzle). The measurements were obtained for both tandem and side-by-side jet configurations, jet spacing of $S/D = 2$ and velocity ratios of $R = 2.2$ and 4.0. Control tests at the same mass flow rate but with uniform exit velocity profiles were also conducted, for comparison purposes.

Some representative results are given here in Fig. Nos. 3 and 4 for 90^{0} injection and $R = 2.2$. These plots show that the effects of exit velocity profile non-uniformity are quite significant.

REFERENCES

1. Schetz, J. A.: Injection and Mixing in Turbulent Flow, AIAA, New York, 1980.

2. Vogler, Raymond D.: Surface Pressure Distirbutions Induced on a Flat Plate by a Cold Air Jet Issuing Perpendicularly From the Plate and Normal to a Low-Speed Free-Stream Flow. NASA TN D-1629, 1963.

3. Vogler, Raymond D.: Interference Effects of Single and Multiple Round or Slotted Jets on a V/STOL Model in Transition. NASA TN D-2380, August 1964.

4. Bradbury, L. J. S.; and Wood, M. N.: The Static Pressure Distributions Around a Circular Jet Exhausting Normally From a Plane Wall Into an Airstream. C. P. No. 822, Brit. A. R. C., 1965.

5. Margason, Richard J.: Jet-Induced Effects in Transition Flight. Conference on V/STOL and STOL Aircraft, NASA SP-116, 1966, pp. 177-189.

6. Gentry, Garl L.; and Margason, Richard J.: Jet Induced Lift Losses on VTOL Configurations Hovering In and Out of Ground Effect. NASA TN D-3166, February 1966.

7. Soullier, A.: Testing at SI. MAS for Basic Investigation on Jet Interactions. Distributions of Pressures Around the Jet Orifice. NASA TTF-14066, April 1968.

8. Fricke, L. B.; Wooler, P. T.; and Ziegler, H.: A Wind Tunnel Investigation of Jets Exhausting Into a Crossflow. AFFDL-TR-70-154, Vols. I-IV, U. S. Air Force, Dec. 1970.

9. Margason, Richard J.: Review of Propulsion-Indiced Effects on Aerodynamics of Jet/STOL Aircraft. NASA TN D-5617, February 1970.

10. Fearn, R. L. and Weston, R. P., "Induced Pressure Distribution of a Jet in a Crossflow," NASA TN D-7916, June 1975.

11. Taylor, P., "An Investigation of an Inclined Jet in a Crosswind," Aeronautical Quarterly, Vol. XXVIII, Part I, February 1977.

12. Kuhlman, J. M., Ousterhout, D. S., and Warcup, R. W.: Experimental Investigation of Effects of Jet Decay Rate on Jet-Induced Pressures on a Flat Plate: Tabulated Data. NASA CR-158990, Nov. 1978.

13. Lee, C. C.: A Review of Research on the Interaction of a Jet With an External Stream, Tech. Note R-184, (Contract No. DA-01-021-AMC-11528 (z)), Res. Lab., Brown Engineering Co., Inc., Mar. 1966. (Available from DDC as AD 630 294).

14. Garner, Jack E.: A Review of Jet Efflux Studies Application to V/STOL Aircraft. AEDC-TR-67-163, U. S. Air Force, Sept. 1967. (Available from DDC as AD 658-432).

15. Perkins. S. C., Jr. and Mendenhall, M. R.: "A Study of Real Jet Effects on the Surface Pressure Distribution Induced by a Jet in a Crossflow," NASA CR-166150, Mar. 1981.

16. Margason, Richard J.: The Path of a Jet Directed at Large Angles to a Subsonic Freestream. NASA TN D-4919, November 1968.

17. Ziegler, H. and Wooler, P. T.: Analysis of Stratified and Closely Spaced Jets Exhausting into a Crossflow. NASA CR-132297, Nov. 1973.

18. Ousterhout, D. S.: An Experimental Investigation of a Cold Jet Emitting from a Body of Revolution into a Subsonic Free Stream. NASA CR-2089, July 1972.

19. Schetz, J. A. and Jakubowski, A. K., "Experimental Study of Surface Pressures Induced on a Flat Plate and a Body of Revolution by Various Dual Jet Configurations. NASA CR- 166422, December 1982.

20. Abramovich, G. N.: The Theory of Turbulent Jets. M.I.T. Press Co., 1963, pp. 541-552.

21. Wu, J. C.; and Wright, M. A.: A Blockage-Sink Representation of Jet Interference Effects for Noncircular Jet Orifices. Analysis of a Jet in a Subsonic Crosswind, NASA SP-218, 1969, pp. 85-99.

22. Street, Troy, A.; and Spring, Donald, J.: Experimental Reaction Jet Effects at Subsonic Speeds. Analysis of a Jet in a Subsonic Crosswind, NASA SP-218, 1969, pp. 63-83.

23. Dietz, W. E., Jr.: A Method for Calculating the Induced Pressure Distribution Associated with a Jet in a Crossflow. M. S. Thesis, Florida University, 1975 (also available as NASA CR 146434, 1975).

24. Yen, K. T., "The Aerodynamics of a Jet in a Crossflow," NADC-78291-60, December 1978.

25. Perkins, S. C., Jr. and Mendenhall, M. R., "A Correlation Method to Predict the Surface Pressure Distribution on an Infinite Plate or a Body of Revolution from which a Jet is Issuing," NASA CR 152345, January 1980.

26. Fearn, R. L., Kalota, C., and Dietz, W. E., Jr., "A Jet Aerodynamic Surface Interference Model," Proceedings V/STOL Aircraft Aerodynamics, Vol. 1, Naval Post Graduate School, Monterey, California, May 1979.

27. Campbell, J. F. and Schetz, J. A.: Analysis of the Injection of a Heated Turbulent Jet into a Cross Flow, NASA TR R-413, Dec. 1973.

28. Baker, A. J., Manhardt, P. E. and Orzechowski, J. A.: A Three-Dimensional Finite Element Algorithm for Prediction of V/STOL Jet-Induced Flowfields, AGARD Symposium, Lisbon, Portugal, Nov. 1981.

29. Isaac, K. M. and Schetz, J. A.: Analysis of Multiple Jets in a Cross-flow, ASME Paper 82-WA/FE-4, Nov. 1982.

ORIGINAL PAGE IS
OF POOR QUALITY

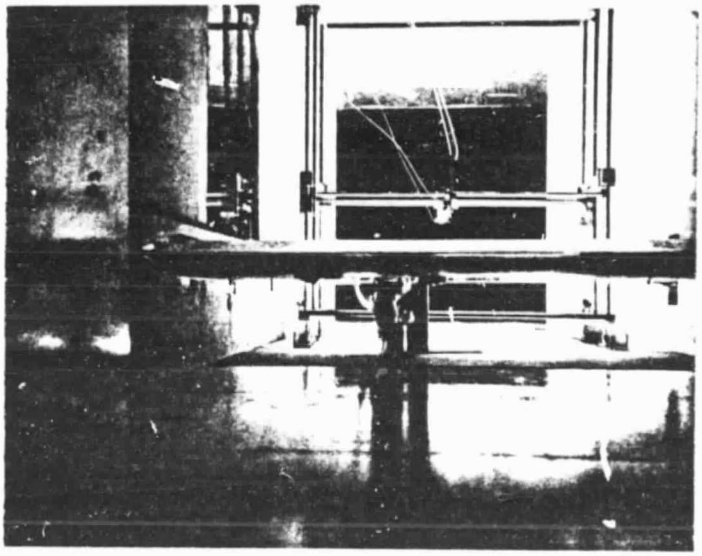

Fig. 1 - Flat Plate Model in the VPI
Wind Tunnel (looking upstream)

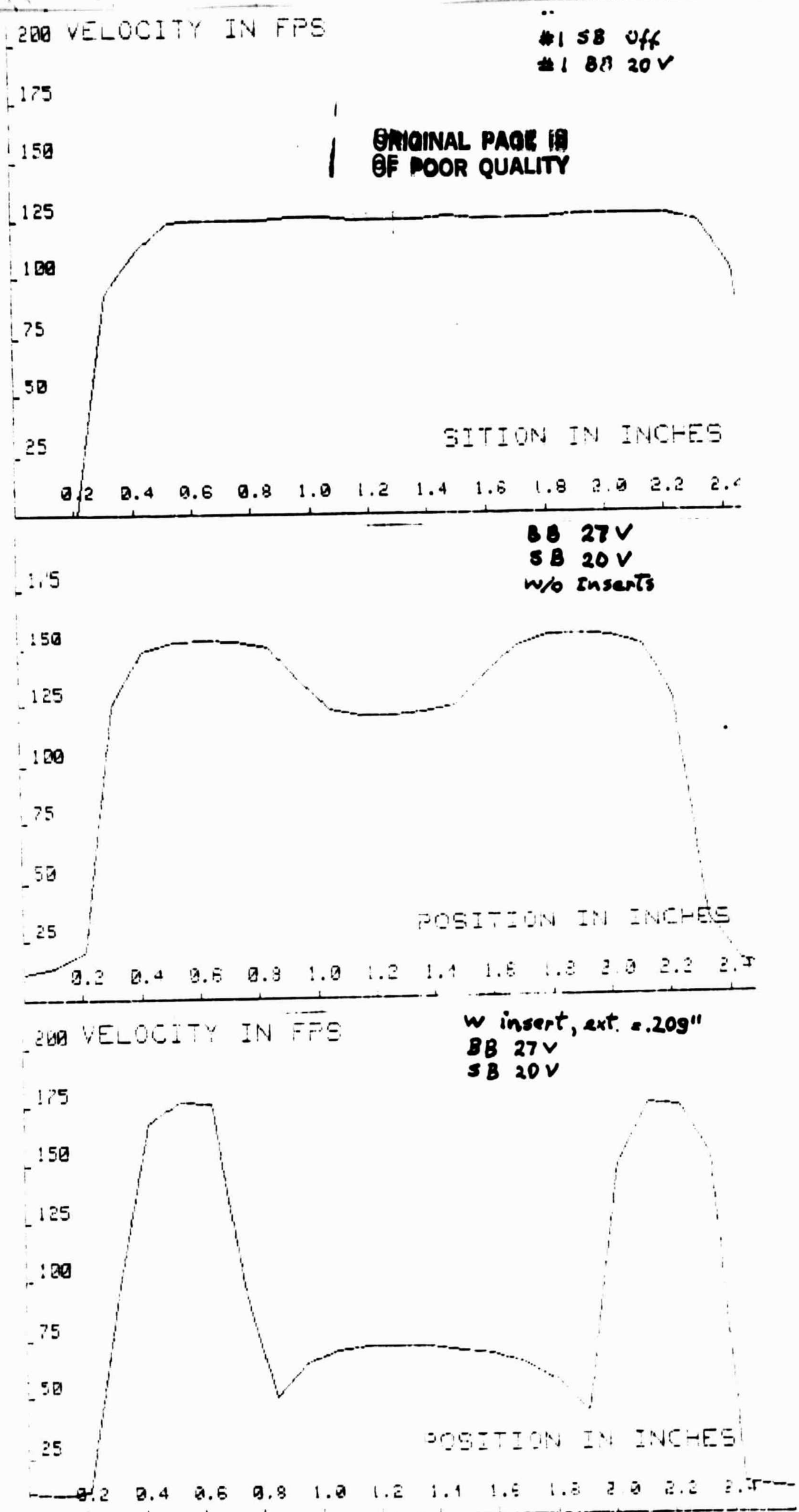

Fig. 2 - Typical Exit Velocity Profiles Obtainable with Modified Injector

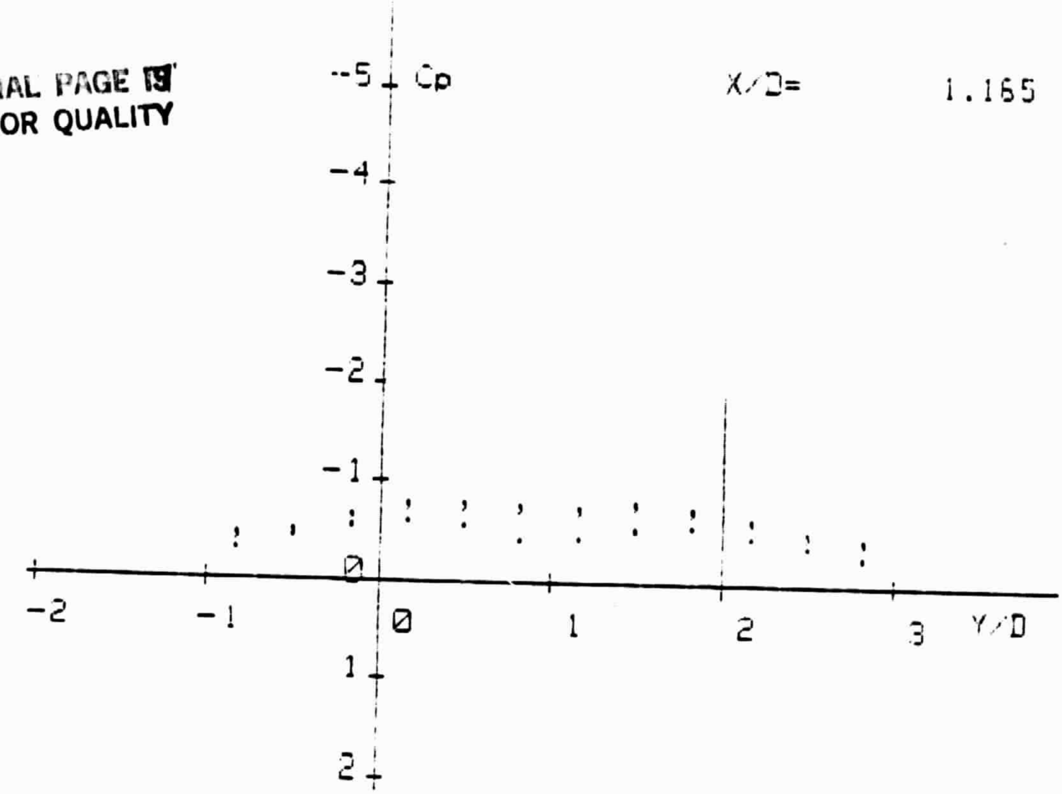

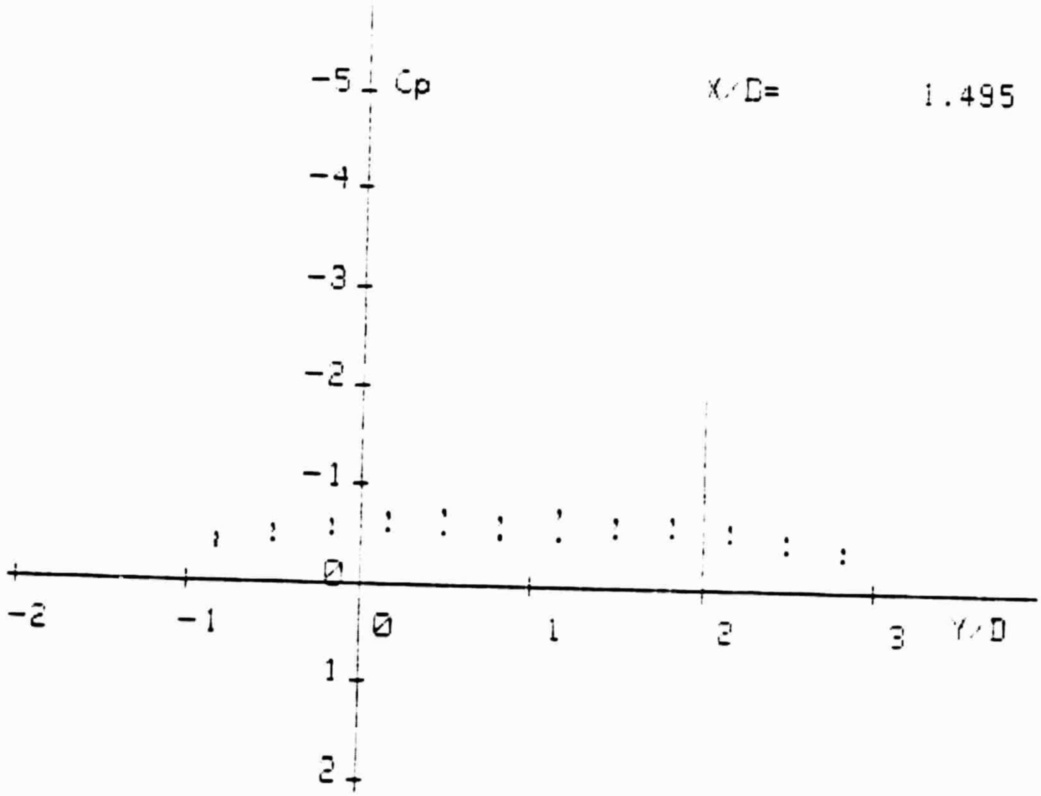

Fig. No. 3 - Pressure Coefficient Plots for 90^o side-by-side Jets, R = 2.2: (•) Uniform Velocity Profile, (•) Non-uniform Velocity Profile.

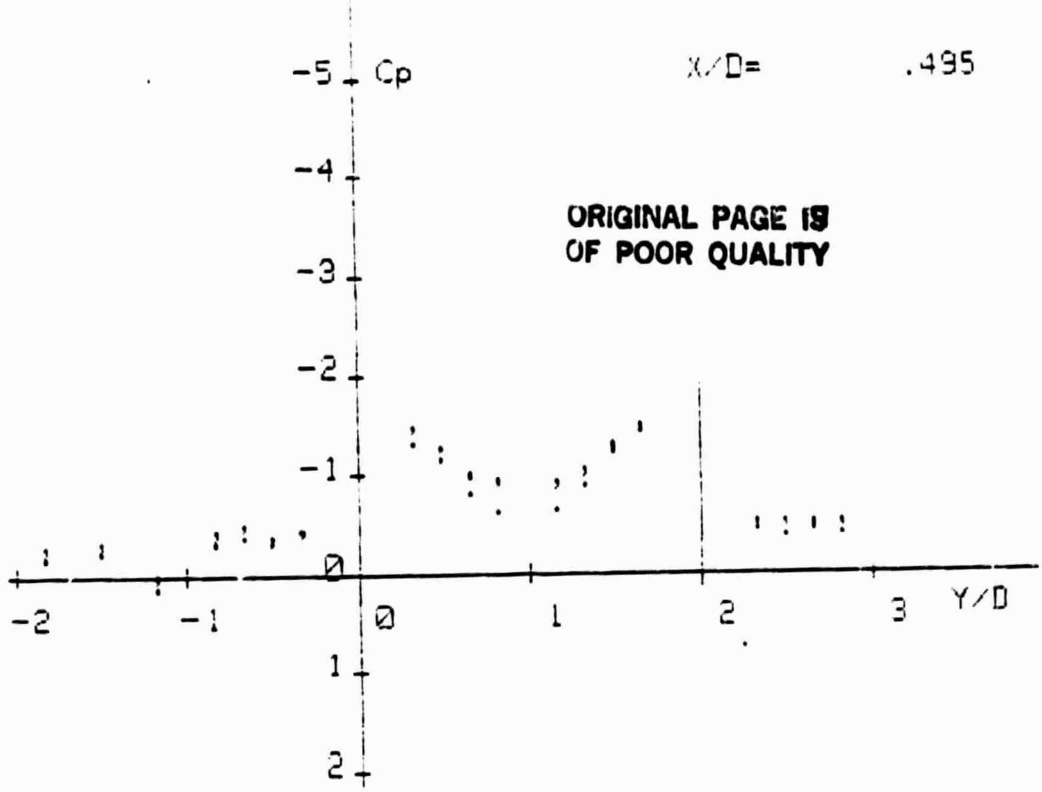

ORIGINAL PAGE IS
OF POOR QUALITY

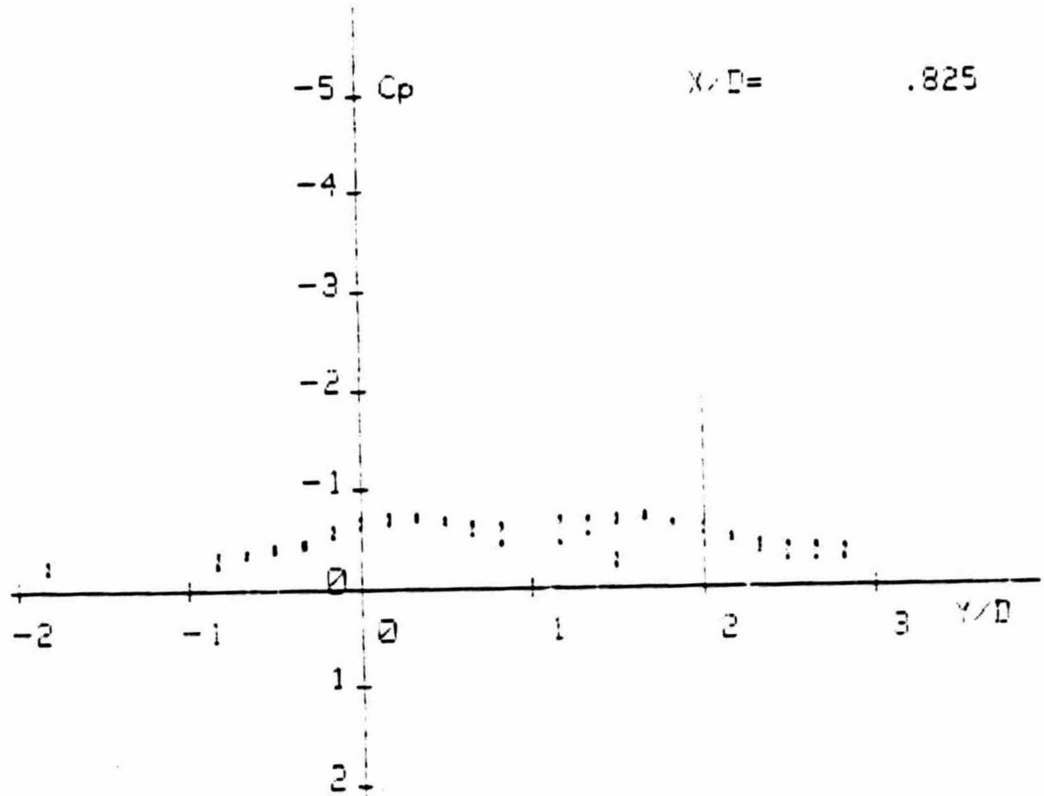

Fig. No. 3 - cont'd.

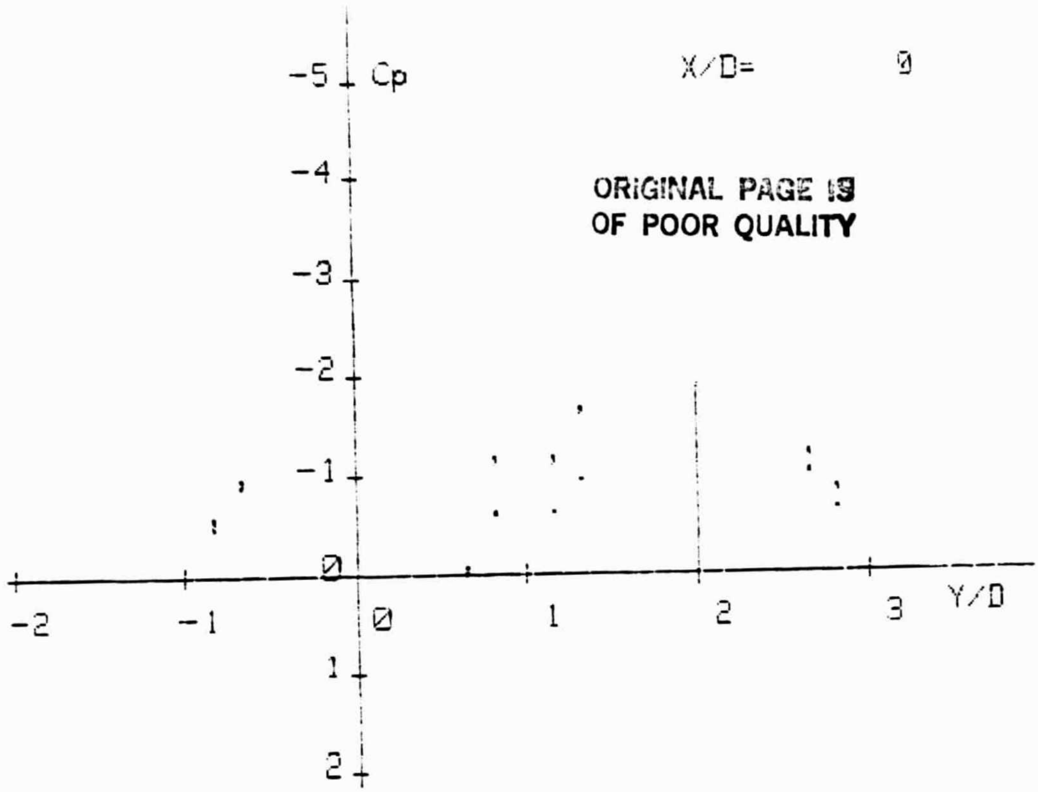

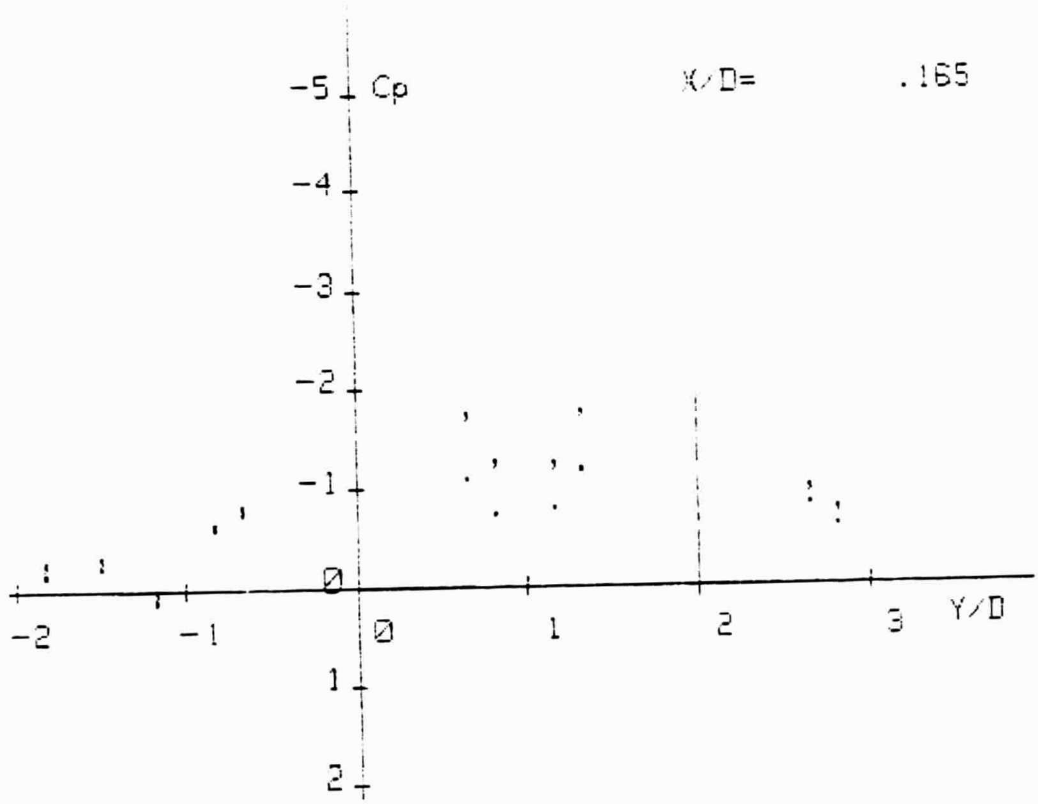

Fig. No. 3 - cont'd.

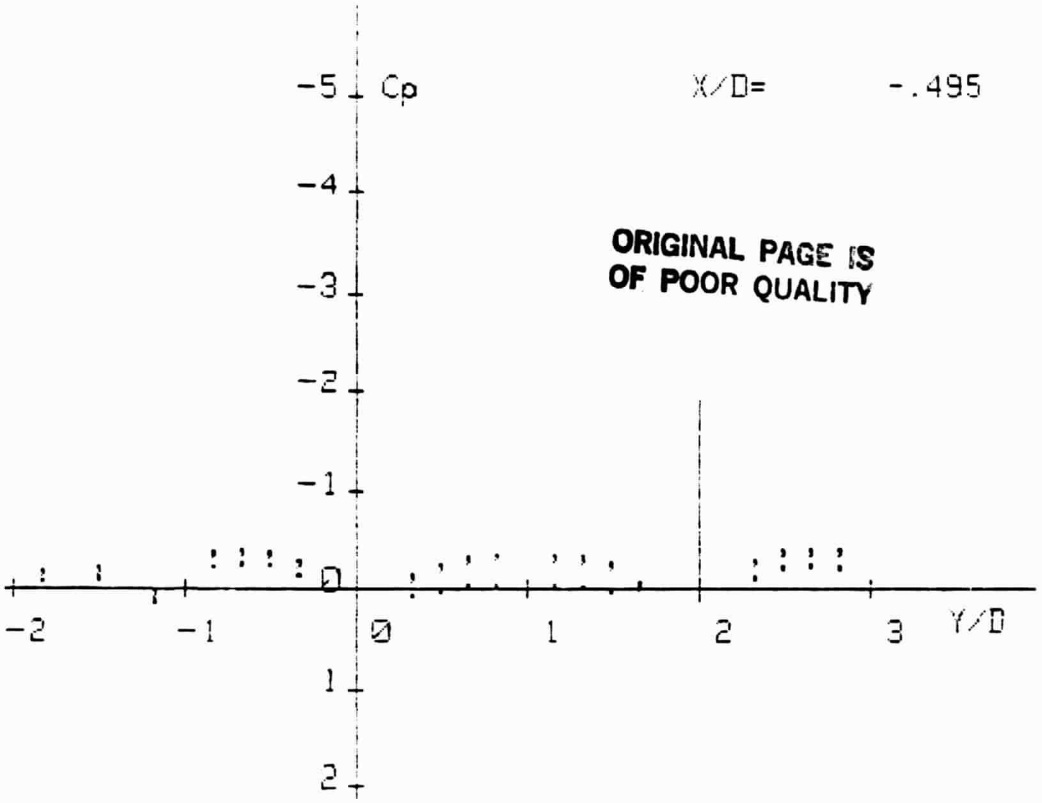

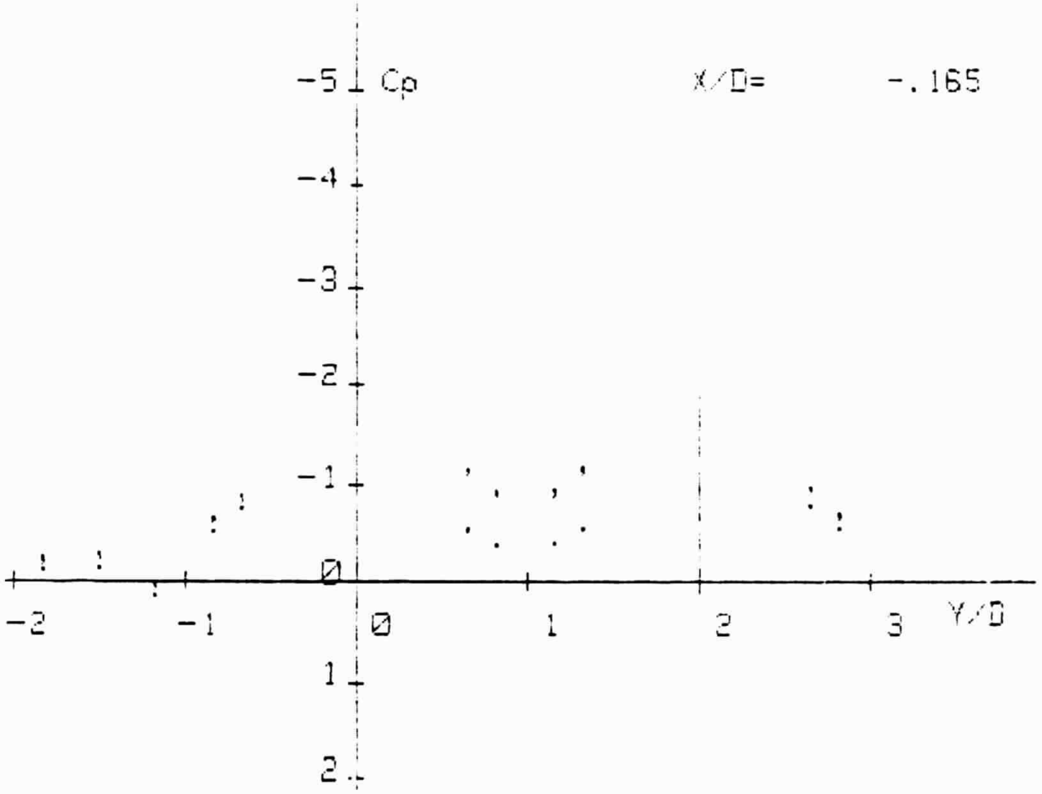

Fig. No. 3 - cont'd.

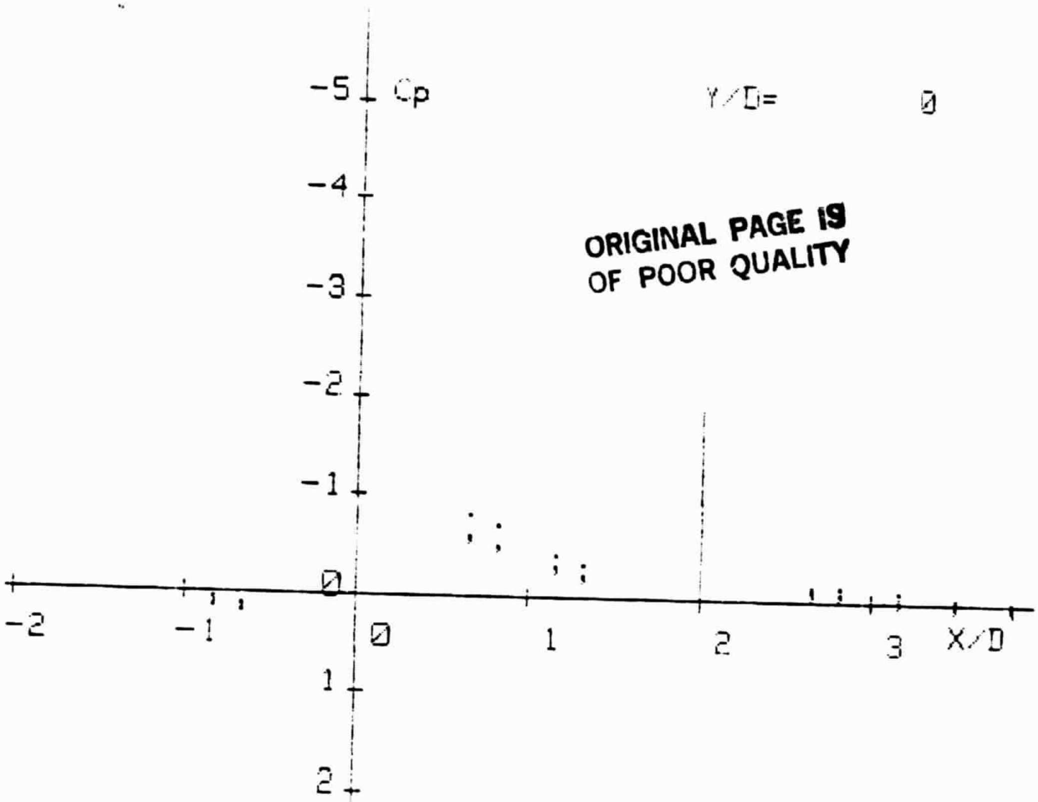

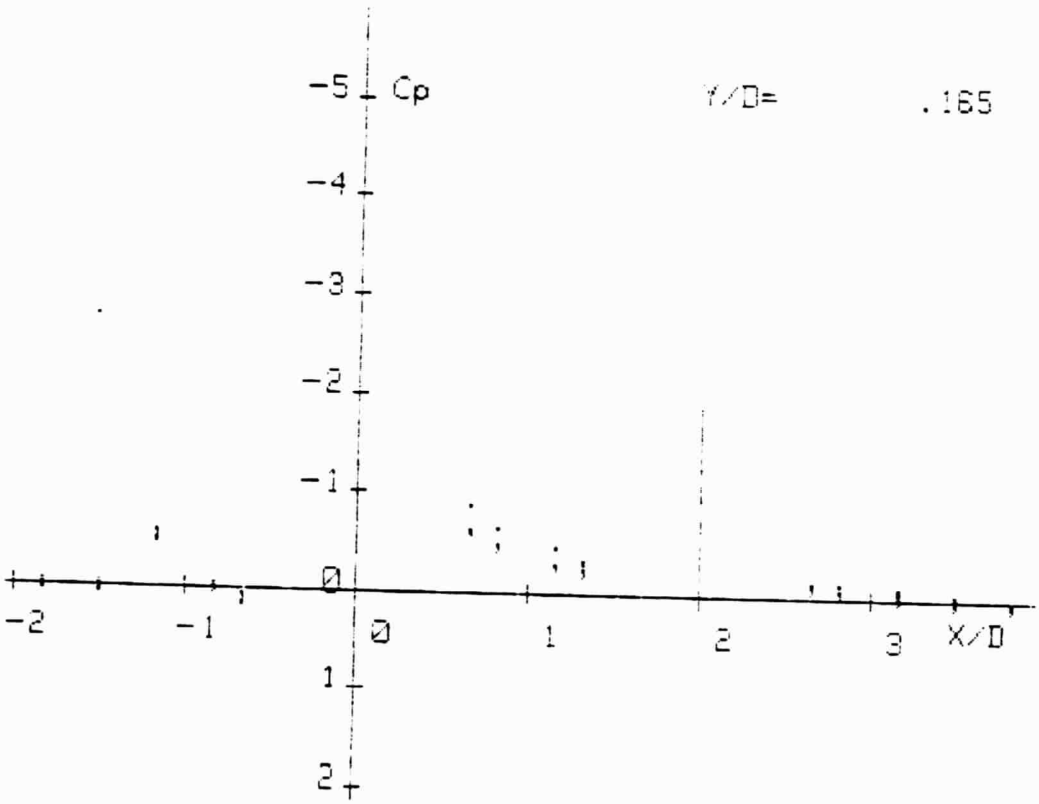

Fig. No. 4 - Pressure Coefficient Plots for 90^o In-Line Jets, R = 2.2: (·) Uniform Velocity Profile, (,) Non-uniform Velocity Profile.

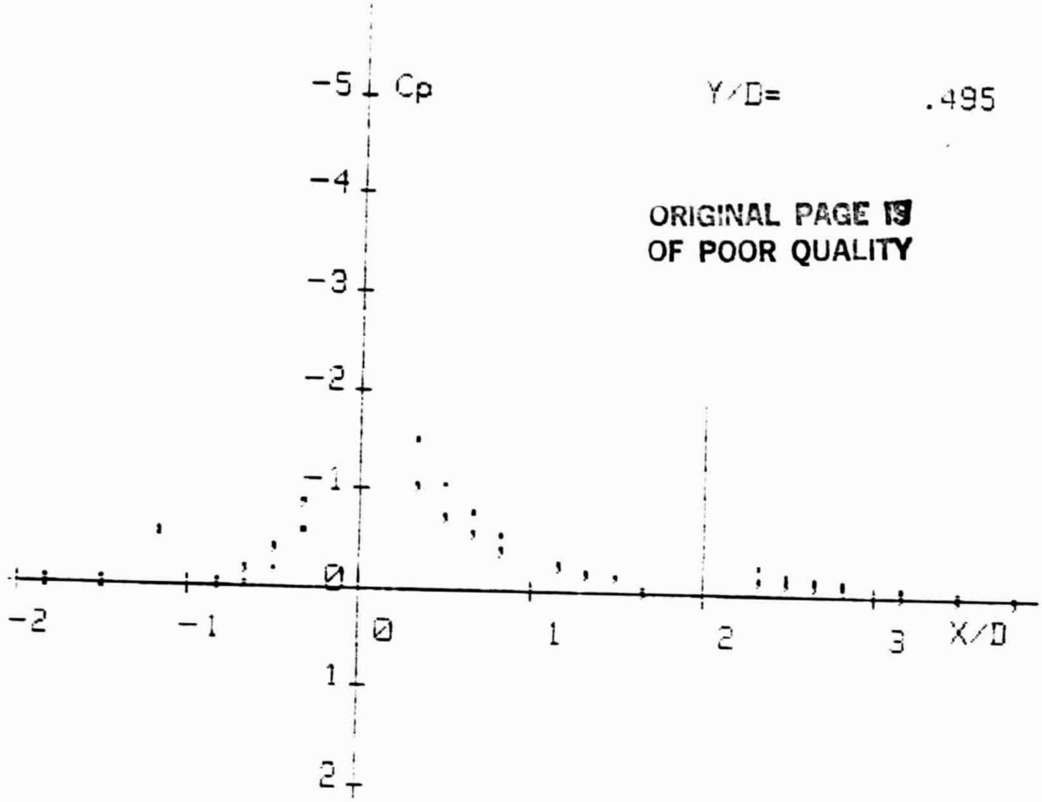

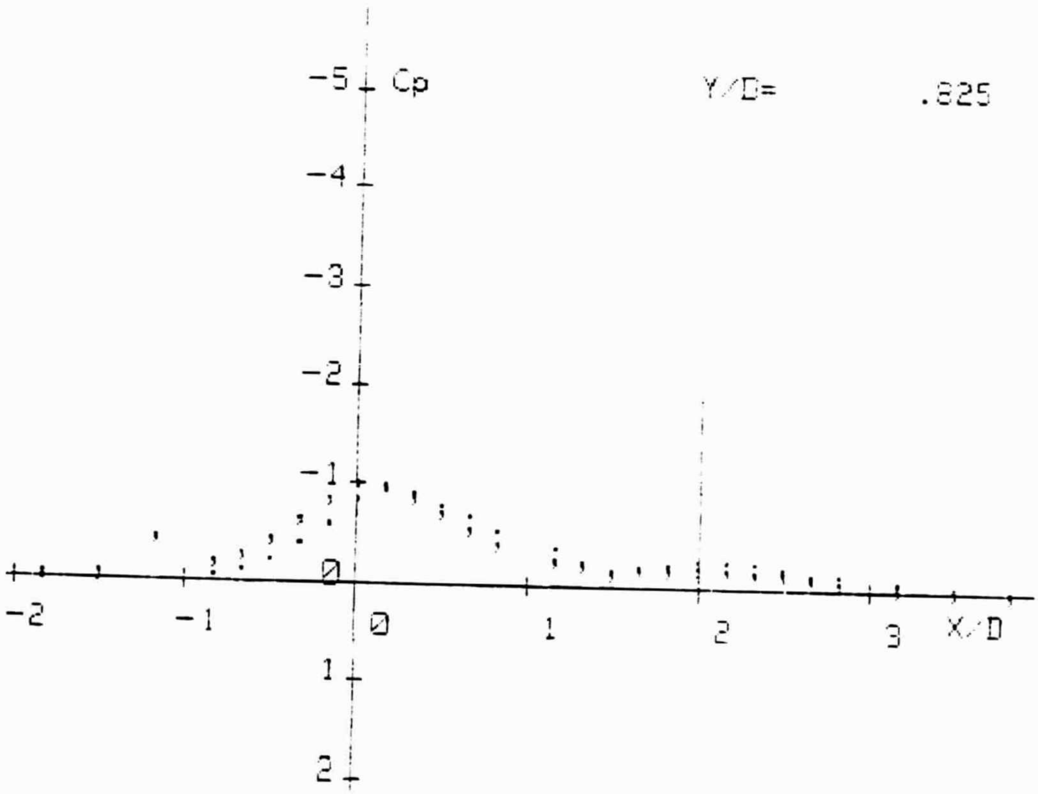

Fig. No. 4 - cont'd.

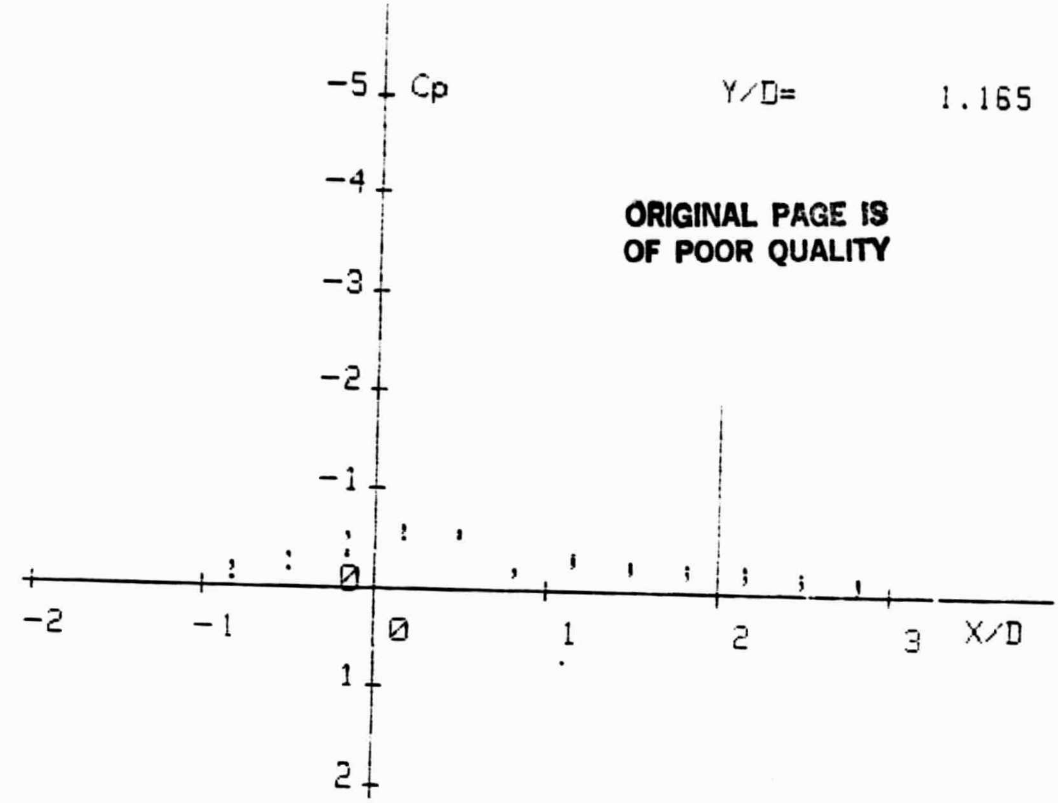

ORIGINAL PAGE IS
OF POOR QUALITY

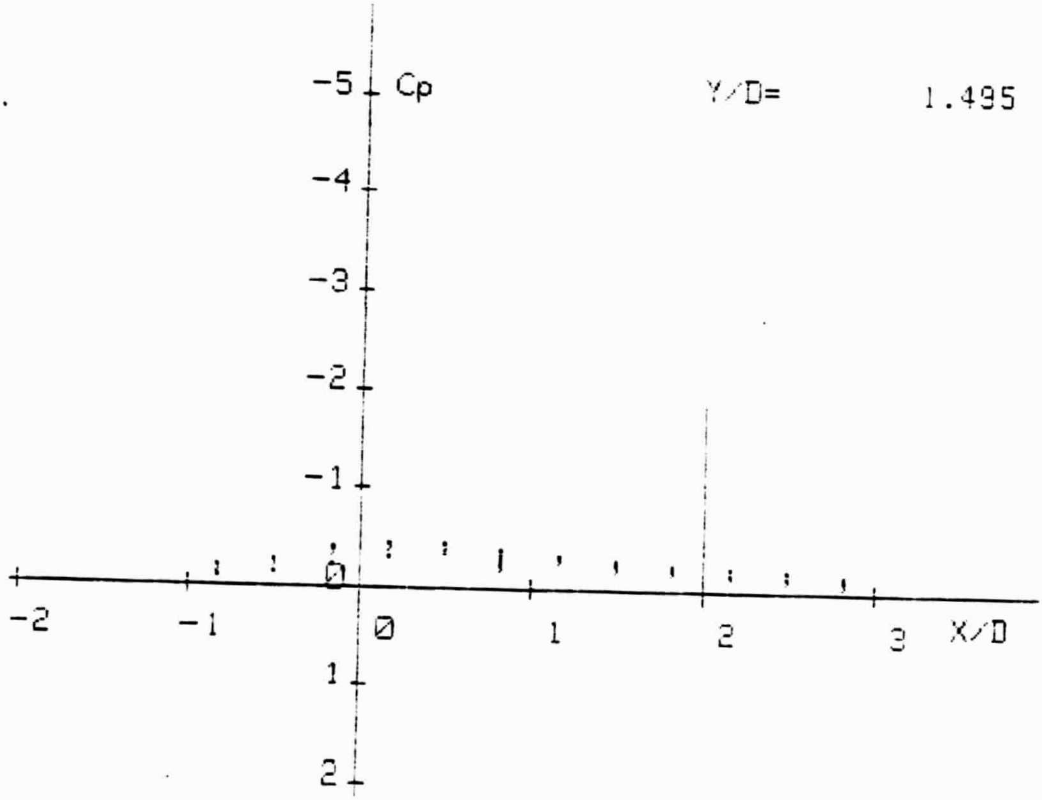

Fig. No. 4 - cont'd.

2qT

Quarterly Status and Technical Progress Report

Landsat-D Thematic Mapper Image Dimensionality Reduction and Geometric Correction Accuracy

NASA Contract Number NAS5-27577

Principal Investigator
Gary E. Ford
Department of Electrical and Comp...er Engineering
University of California, Davis
Davis, California 95616

(E84-10149) LANDSAT-D THEMATIC MAPPER IMAGE DIMENSIONALITY REDUCTION AND GEOMETRIC CORRECTION ACCURACY Quarterly Status Technical Progress Report, 3 Dec. 1983 - 3 Mar. 1984 (California Univ.) 7 p N84-26097 Unclas G3/43 00149

For the period: December 3, 1983 to March 3, 1984

1. Problems

The progress of the investigation has been impeded during this reporting period by the heavy teaching and graduate advising load of the principal investigator. Approval has been obtained to take a leave of absence to devote full time to this project for the remainder of the contract period.

2. Accomplishments

The thematic mapper scene that is the most useful in our investigation was received during the reporting period. This is a scene from path 27, row 39 of central Texas (Scene ID E-40193-16315, acquired January 25, 1983), covering the Walnut Creek watershed east of Austin, Texas. We have studied this watershed previously for the U.S. Army Corps of Engineers (Ford, et al., 1983) using MSS data. We have a substantial collection of ground truth data for this study area, including color infrared aerial photography, USGS topographic maps, and the results of manual and computer classification studies.

We have made a preliminary study of a 1024 by 1024 subscene of this image, centered on Austin, Texas. The ranges of intensity values in all of the TM bands were found to be substantially greater than those we had observed in the other TM image available to us, a February 2, 1983 acquisition centered near Sacramento, California. Since both of these images were acquired during the winter months, the low sun angle would be expected to produce low dynamic ranges. However, we are unable to provide an explanation as to why there is such a disparity between the two images, acquired just seven days apart. We observed a 50% increase in standard deviation in the intensities in bands 1, 2, 3, 5, and 7; no change in band 4; and a 25% decrease in band 6. The decrease in the thermal band is probably due to the low percentage of water in the Texas image. Due to the heavy rainfall in California during the 1982-83 winter, the study area of interest to us on the Sacramento River was extensively flooded on the date of acquisition of the image and we are unable to perform a classification study on this image. While the late January date is not the optimum for a classification study of the Walnut Creek watershed, an interactive analysis of the image shows that the major land use classes exhibit spectral separation.

Principal components transformation has been applied to the Walnut Creek subscene to reduce the dimensionality of the multispectral sensor data. The results are summarized in Table 1. For comparison purposes, we have also applied this transformation to a Landsat 3 MSS subscene of the same area. The MSS scene was acquired in a different season and year (May 1978), but the results, as summarized in Table 2, allow for comparisons between TM and MSS data.

The correlation matrices indicate the pairwise correlation of the spectral components. The TM correlation matrix shows that visible bands 1-3 exhibit a high degree of correlation, in the range 0.92 to 0.96. While it might be expected that the reflective infrared bands 4, 5, and 7 would be highly correlated, this is only true for bands 5-7, where the correlation is 0.93. Band 4 is not highly correlated with any other band, with correlations in the range 0.13 to 0.52. Similarly, the thermal band 6 is not highly correlated with other bands, with correlations in the range 0.13 to 0.46. It should be noted that bands 1-3 exhibit a moderate degree of correlation with bands 5 and 7, with correlations in the range 0.63 to 0.83. These results are significantly different than those we reported for the Sacramento subscene in our project report for the period June 3, 1983 to September 3, 1983. This is a further indication that the Sacramento scene is not representative of data from the TM sensor.

The MSS correlation matrix shows that the visible bands (4 and 5) are highly correlated (0.96), as are the reflective infrared bands (6 and 7), with a correlation of 0.92. On the basis of this comparison between TM and MSS data, we are unable to support the expectation that there would be lower correlation among the TM spectral components than has been observed for the MSS spectral components.

The principal components transformation matrix is composed of the normalized eigenvectors of the covariance matrix ordered by eigenvalues. The weights used to generate a transformed component are given in the columns